

AD-A037 257

NORTHROP RESEARCH AND TECHNOLOGY CENTER HAWTHORNE CALIF
OPTICAL COATINGS 2-6 MICRONS.(U)

F/G 11/3

JAN 77 P KRAATZ
NRTC-77-8R

N00123-76-C-1321
NL

UNCLASSIFIED

| OF |
AD
A037257



ADA037257

20



DDC
RECEIVED
MAR 21 1977
A

DISTRIBUTION STATEMENT A
Approved for public release;
Distribution Unlimited

NORTHROP

Research and Technology Center

14
20
NRTC-77-8R
PIN 2271

6
OPTICAL COATINGS 2-6 MICRONS.

9
SEMI-ANNUAL TECHNICAL REPORT.

11
JANUARY 1977

12
55p.

10
Paul Kraatz
Principal Investigator

DISTRIBUTION STATEMENT A

Approved for public release;
Distribution Unlimited

DDC
RECEIVED
MAR 21 1977
RECEIVED

Prepared For

Naval Weapons Center

Contract No. N00123-76-C-1321 *new*

15
By

Northrop Research and Technology Center,
3401 West Broadway
Hawthorne, California 90250

407 696 *mt*

OPTICAL COATINGS 2-6 MICRONS
SEMI-ANNUAL TECHNICAL REPORT

TABLE OF CONTENTS

<u>Section</u>	<u>Title</u>	<u>Page</u>
1.	INTRODUCTION	1
2.	MATERIAL PROCUREMENT AND CERTIFICATION. . .	1
3.	SUBSTRATE SURFACE PREPARATION	14
4.	SUBSTRATE ABSORPTANCE MEASUREMENT	19
5.	SUBSTRATE SURFACE CHEMISTRY AND CLEANING. .	33
6.	FUTURE PLANS.	33
7.	REFERENCES	35
APPENDIX		36

ALLOCATION IN

NTIS

000

UNCLASSIFIED

Letter on file

BY

DISSEMINATING/REPLACING CODES

DIR

1961 JAN 10 SPECIAL

A

1. INTRODUCTION

Progress during the first half year (June through December, 1976) under Contract No. N00123-76-C-1321 is reported here. This report incorporates the Second Quarterly Report and Semi-Annual Technical Report in one document. The report is divided into five sections covering material procurement and certification, substrate surface preparation, substrate absorptance measurement, substrate surface chemistry, and future plans.

This report documents results of characterization and testing of substrate and coating materials to be employed in the main thrust of the contractual effort, optimization of coatings for 2-6 μm laser optics. A sizable body of data is assembled and organized for future use in the coating portion of the program. Principal results comprise x-ray diffraction analyses of the coating materials, documentation of substrate surface finish, total absorptance of CaF_2 and SrF_2 substrates at 3.8 and 5.3 μm , and results of a study of substrate surface chemistry as affected by cleaning procedures.

2. MATERIAL PROCUREMENT AND CERTIFICATION

Single crystal CaF_2 and SrF_2 substrates have been ordered from Harshaw Chemical Co., Solon, Ohio. Ninety-One CaF_2 substrates were received between 1 and 15 August 1976. The balance (121 SrF_2 and 40 CaF_2) were received between 26 October and 5 November 1976, approximately one month to six weeks later than planned and necessitating some adjustments in scheduling. Crystallographic orientation of all of these was verified using the back reflection Laue (x-ray) method. Of the CaF_2 substrates having a nominal (111) orientation, 90% fell within 1.5° of that orientation and none was more than 3° from (111). Of the nominal (110) CaF_2 substrates, 99% fell within 2° to 5° of (110) and none were more than 8° from the nominal. Of the (112) substrates, all fell within 2.5 to 5.0° of nominal. Of the (100) CaF_2 substrates, all but one fell within 2° of nominal. All SrF_2 samples of the four orientations, (100), (110), (111), and (112) fell within 3° of the nominal orientations.

Spurious peaks of low intensity were obtained in patterns for five of these materials. In the case of MgF_2 taken from the electron gun boat in the coating unit, all three spurious lines may arise from ThF_4 , indicating contamination within the chamber rather than in the original material. However, two of these three lines may alternatively be ascribed to elemental magnesium, indicating possible non-stoichiometry or dissociation of the compound during deposition.

For MgO , the impurity is identified as MgF_2 (Table 4) and for SrF_2 (Table 6) it is $\text{Sr}(\text{OH})_2$, a common impurity in alkaline earth fluorides due to the similarity of size and charge of the OH^- and F^- ions and the difficulty in scavenging all water and oxygen from fluoride melts. Both of these materials were examined as received. The best fit for the one spurious peak in the ThF_4 (as received material) pattern (Table 7) is Thorium boride, but other possibilities include $\text{ThOCl}_2 \cdot 14 \text{H}_2\text{O}$, $\text{Th}(\text{SO}_4)_2$ and $\text{K Th}_6\text{F}_{25}$. The hydrated oxichloride and sulfate are potentially troublesome, if present in any appreciable quantity, as is the $\text{Sr}(\text{OH})_2$.

In the case of ZnS (Table 10), the spurious peak arises almost certainly from ZnSe ; due to the similarities in structure and physical properties of ZnS and ZnSe , this impurity is not expected to present serious problems.

PRECEDING PAGE BLANK NOT FILMED

Table 1. RESULTS OF X-RAY DIFFRACTION STUDY
OF Al_2O_3 COATING MATERIAL.

Material Source and Conditions: Crystalline fragments from supply.

(Crystal products-end cuttings from Boule of UV grade sapphire)

Material	Card Ref.	Obs. $d(\text{\AA})$	Obs. I/I_{100}	ASTM $d(\text{\AA})$	ASTM I/I_{100}	hkl	Notes
$\alpha\text{-Al}_2\text{O}_3$	10-173	3.483	30	3.479	75	012	
		2.551	38	2.552	90	104	
		2.378	09	2.379	40	110	
		2.085	43	2.085	100	113	
		1.737	60	1.740	45	024	
		1.600	100	1.601	80	116	
		1.404	46	1.404	30	124	
		1.376	11	1.374	50	030	
		1.1921	06	1.1898	07	220	
		1.0780	15	1.0781	07	134	
$\theta\text{-Al}_2\text{O}_3$	11-517	2.812	17	2.85	80	004	
		1.773	06	1.80	30	015	

Table 2. RESULTS OF X-RAY DIFFRACTION STUDY
OF BaF₂ COATING MATERIAL.

Material Source and Condition: Residual from E-Gun boat. Supplier: EMCO

Material	Card Ref.	Obs. d(Å)	Obs. I/I ₁₀₀	ASTM d(Å)	ASTM I/I ₁₀₀	hkl	Notes
BaF ₂	4-0452	3.559	100	3.579	100	111	
		3.087	17	3.100	30	200	
		2.184	49	2.193	79	220	
		1.864	47	1.870	51	311	
		1.784	13	1.790	03	222	
		1.545	06	1.550	06	400	
		1.418	09	1.423	13	331	
		1.383	07	1.386	06	420	
		1.262	08	1.266	14	422	
		1.191	08	1.193	06	511	
		1.0951	08	1.0959	02	440	
		1.0464	06	1.0481	06	531	
		1.0320	07	1.0332	< 1	600	

Table 3. RESULTS OF X-RAY DIFFRACTION STUDY
OF MgF_2 COATING MATERIAL.

Material Source and Condition: Residual from E-Gun boat. Balzers >99.9%

Material	Card Ref.	Obs. $d(\text{\AA})$	Obs. I/I_{100}	ASTM $d(\text{\AA})$	ASTM I/I_{100}	hkl	Notes
MgF_2	6-0290	3.264	100	3.265	100	100	
		2.547	11	2.545	22	101	
		2.231	59	2.231	96	111	
		2.067	22	2.067	34	210	
		1.710	90	1.711	73	211	
		1.633	42	1.635	31	220	
		1.527	35	1.526	19	002	
		1.461	06	1.462	06	310	
		1.375	34	1.375	35	301	
		1.317	04	1.318	07	311	
		1.281	01	1.282	01	320	
		1.227	02	1.228	06	212	
		1.114	08	1.115	10	222	
		1.0888	47	1.0893	06	330	
		1.0523	06	1.0524	06	411	
		1.0324	02	1.0333	02	420	
ThF_4	23-1426	3.6085	04	3.63	50	312	
		2.4694	03	2.495	10	231	1
		1.8940	03	1.881	10	350	

1. Elemental Mg (101) and (102) lines are also possible sources of the last
2 peaks. For Mg (101) $d = 2.453\text{\AA}$, $I = 100$; for Mg (102) $d = 1.901\text{\AA}$.
 $I = 20$.

Table 4. RESULTS OF X-RAY DIFFRACTION STUDY
OF MgO COATING MATERIAL.

Material Source and Condition: Supply - Balzers Ch 73-085/2

Material	Card Ref.	Obs. d (Å)	Obs. I/I ₁₀₀	ASTM d (Å)	ASTM I/I ₁₀₀	hkl	Notes
MgO	4-0289	2.427	11	2.431	10	111	
		2.106	100	2.106	100	200	
		1.488	53	1.489	52	220	
		1.269	06	1.270	04	311	
		1.215	14	1.216	12	222	
		1.0523	05	1.0533	05	400	
α -MgF ₂	16-160	2.330	04	2.261	20	222, 410	1
		1.6474	03	1.647	70	440	

1. Best fit of probable Mg compounds; i.e., other oxides, hydroxides,
and fluorides.

Table 5. RESULTS OF X-RAY DIFFRACTION STUDY
OF PbF_2 COATING MATERIAL.

Material Source and Condition: Residual material from boat. Balzers >99.9%

Material	Card Ref.	Obs. $d(\text{\AA})$	Obs. I/I_{100}	ASTM $d(\text{\AA})$	ASTM I/I_{100}	hkl	Notes
αPbF_2	6-0288	3.76	05	3.824	10	002	Over- laps w/ βPbF_2 (422) ²
		3.27	07	3.290	100	012	
		1.2000	09	1.2079	04	151	
βPbF_2	6-0251	3.411	100	3.428	100	111	
		2.954	32	2.970	56	200	
		2.092	59	2.100	73	220	
		1.786	42	1.791	64	311	
		1.709	7	1.715	14	222	
		1.481	8	1.485	10	331	
		1.325	8	1.328	21	420	
		1.2000	9	1.212	26	422	
		1.1406	8	1.143	20	511	
		1.0483	5	1.050	8	440	
		1.0026	8	1.0043	20	531	
		0.9890	4	0.9903	13	600	

Table 6. RESULTS OF X-RAY DIFFRACTION STUDY
OF SrF_2 COATING MATERIAL.

Material Source and Condition: EMCO Lot 76437/1458 (Crystal Fragments,
as received, ground).

Material	Card Ref.	Obs. $d(\text{\AA})$	Obs. I/I_{100}	ASTM $d(\text{\AA})$	ASTM I/I_{100}	hkl	Notes
SrF_2	6-0262	3.298	100	3.352	100	111	
		2.891	05	2.900	25	200	
		2.045	74	2.051	80	220	
		1.7446	18	1.7486	52	311	
		1.6703	5	1.6743	5	222	
		1.4455	3	1.4499	15	400	
		1.3273	8	1.3303	21	331	
		1.2949	2	1.2966	10	420	
		1.1818	6	1.1840	24	422	
		1.1146	2	1.1164	16	511	
		1.0245	2	1.0253	7	440	
		0.9799	5	0.9803	14	531	
		0.9657	18	0.9666	7	600	
		0.9163	4	0.9170	10	620	
$\text{Sr}(\text{OH})_2$	{18-1273} {19-1276}	3.6896	04	{3.85} {3.65}	80 75	210 n.i.	

Table 7. RESULTS OF X-RAY DIFFRACTION STUDY
OF ThF₄ COATING MATERIAL.

Material Source and Condition: Supply Cerac TS-106 5466

Material	Card Ref.	Obs. d(Å)	Obs. I/I ₁₀₀	ASTM d(Å)	ASTM I/I ₁₀₀	hkl	Notes
ThF ₄	23-1426	7.59	14	7.63	10	110	
		5.24	11	5.24	10	200	
		4.297	81	4.29	80	20 $\bar{2}$	
		4.019	58	4.02	60	3 $\bar{1}1$	
		3.806	100	3.80	100	220	
		3.630	51	3.63	50	312	
		3.354	34	3.35	50	310	
		2.855	08	2.848	05	102	
		2.736	15	2.747	15	13 $\bar{2}$	
		2.533	07	2.528	10	311	
		2.496	10	2.495	10	231	
		2.162	22	2.156	15	430	
		2.130	83	2.132	35	13 $\bar{3}$	
		2.063	17	2.067	05	50 $\bar{4}$	
		2.030	22	2.040	20	20 $\bar{4}$	
		1.984	22	1.985	35	611	
		1.932	12	1.937	15	312	
		1.770	14	1.771	10	63 $\bar{1}$	
		1.576	12	1.585	10	644	
		1.436	46	1.431	10	645	
ThB ₆₆	21-1220	6.752	08	6.799			1
ThF ₄	15-413	3.167	52	3.15	10	n.i.	

1. Other possibilities include ThOCl₂ · 14 H₂O (6.706Å), Th (SO₄)₂ · 9H₂O (6.90Å), and KTh₆ (6.928Å).

Table 8. RESULTS OF X-RAY DIFFRACTION STUDY
OF ThO₂ COATING MATERIAL.

Material Source and Condition: Supply (99.9% Typical) Cerac

Material	Card Ref.	Obs. d (Å)	Obs. I/I ₁₀₀	ASTM d (Å)	ASTM I/I ₁₀₀	hkl	Notes
ThO ₂	4-0556	3.229	100	3.234	100	111	
		2.794	27	2.800	35	200	
		1.975	62	1.980	58	220	
		1.685	54	1.689	64	311	
		1.614	10	1.616	11	222	
		1.408	10	1.400	08	400	
		1.282	27	1.284	26	331	
		1.250	19	1.252	17	420	
		1.1412	13	1.1432	20	422	
		1.0753	12	1.0779	19	511	

Table 9. RESULTS OF X-RAY DIFFRACTION STUDY
OF ZnSe COATING MATERIAL.

Material Source and Condition: Balzers 72-190/12 (As Received)

Material	Card Ref.	Obs. d(Å)	Obs. I/I ₁₀₀	ASTM d(Å)	ASTM I/I ₁₀₀	hkl	Notes
β-ZnSe (Cubic)	5-0522	3.276	94	3.273	100	111	
		2.004	100	2.003	70	220	
		1.710	87	1.707	44	311	
		1.414	14	1.416	09	400	
		1.2995	22	1.299	13	331	
		1.1562	14	1.1561	15	422	
		1.0900	07	1.0901	08	511	
		1.0011	07	1.0018	04	440	
		0.9576	08	0.9577	08	531	
α-ZnSE (Hex)	15-105	3.483	03	3.43	100	100	

Table 10. RESULTS OF X-RAY DIFFRACTION STUDY
OF ZnS COATING MATERIAL.

Material Source and Condition: Supply Balzers Ch 73-027/5 as received.

Material	Card Ref.	Obs. d(Å)	Obs. I/I ₁₀₀	ASTM d(Å)	ASTM I/I ₁₀₀	hkl	Notes
d-ZnS (Hex)	5-0492	3.300	34	3.309	100	100	
		3.118	100	3.128	86	002	
		2.924	22	2.925	84	101	
		2.266	06	2.273	29	102	
		1.909	68	1.911	74	110	
		1.763	11	1.764	52	103	
		1.627	44	1.630	45	112	
		1.598	05	1.599	12	201	
		1.350	04	1.351	06	400	
		1.2965	05	1.296	14	203	
		1.1018	09	1.1029	13	300	
		1.0397	07	1.0401	05	302	
α-ZnSe	15-105	3.450	04	3.43	100	100	
α-ZnS (Polytype)	12-688	2.111	04	2.08	02	---	
β-ZnS	5-0566	2.700	05	2.705	10	200	
		1.350	04	1.351	06	400	
		1.239	06	1.240	09	331	

3. SUBSTRATE SURFACE PREPARATION

All of the 1.00 inch and 1.52 inch diameter single crystal CaF_2 and SrF_2 samples have been polished and characterized using Nomarski microscopy. The optical finishing technique is basically a three-step process in which the window substrate is initially ground flat on a cast iron lap using $9\text{ }\mu\text{m}$ Al_2O_3 abrasive in a water vehicle. To remove the light scratches and pits remaining from the grinding operation, the window substrate is given a rough polish on a pitch lap with $1\text{ }\mu\text{m}$ Al_2O_3 (Linde C) in a water vehicle. The surface is considered ready for the final polishing when visual inspection with a 7 x loupe reveals that all grinding marks have been removed. The window is then finished to the required flatness and surface quality on a medium hard pitch lap (Swiss pitch #73) with $0.3\text{ }\mu\text{m}$ Al_2O_3 (Linde A) in de-ionized water using a recirculating slurry system (a modified bowl feed technique). The window is polished until optimum surface finish is obtained as judged by Nomarski microscopy examination.

Examples of the quality of polished surfaces achieved on CaF_2 and SrF_2 are illustrated in Figures 1 through 5. Note that all surfaces are relatively free of defects, indicating that polishing behavior does not vary significantly with crystallographic orientation, as long as samples of a single orientation are polished on one block. In order to investigate this further, samples will be submitted to the Michelson Laboratory, NWC, for surface roughness evaluation and quantitative documentation.

In a previous study,⁽¹⁾ it was found that when substrates having (100), (110), and (111) orientations are polished simultaneously on the same, effectively rigid block, the (100) and (110) surfaces polish well and the (111) surface exhibits appreciable scratching. It was postulated that the observed differences in surface quality resulted from different rates of material removal from the (111) and (100) or (110) surfaces, the rate of removal from the (111) surface being most rapid, due to the natural cleavage in this plane. In that study, segregating and blocking substrates according to orientation

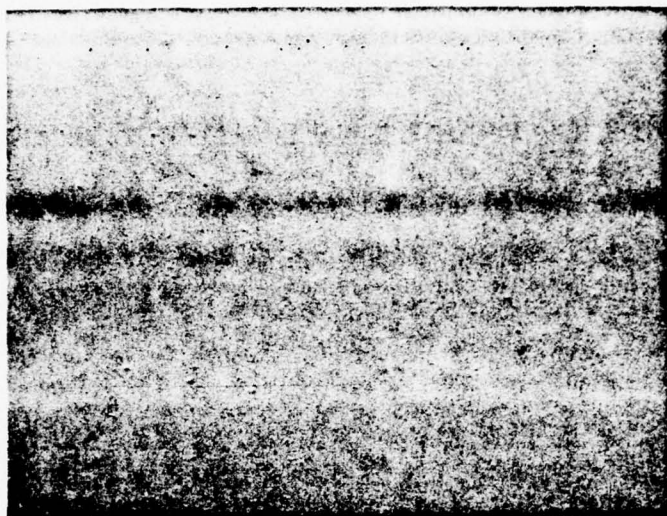


Figure 1. Polished-surface of CaF_2 oriented parallel to the (111) crystallographic plane. Nomarski photomicrograph, 305X, Sample No. (111)-20.



Figure 2. Polished surface of CaF_2 oriented 2.5° from the (110) crystallographic plane. Nomarski photomicrograph, 305X, Sample No. (110)-27.

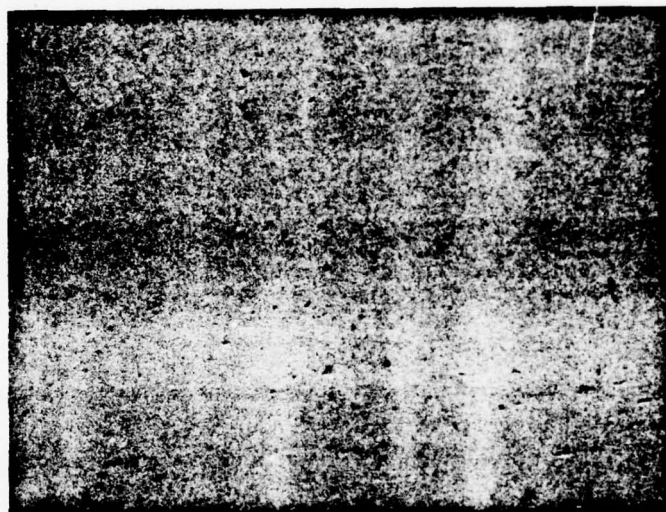
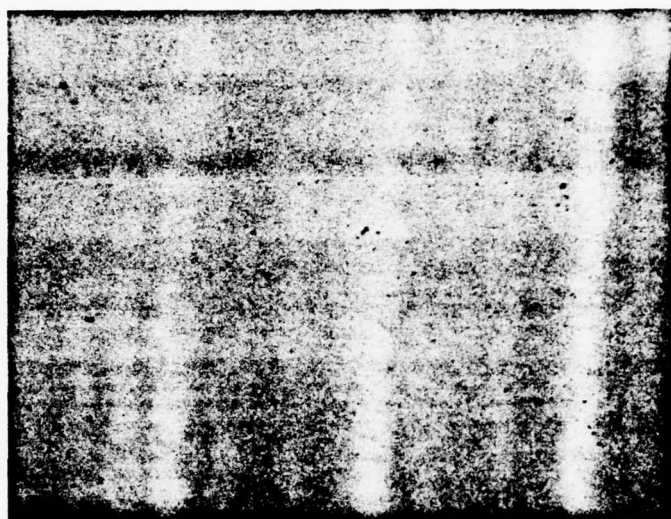
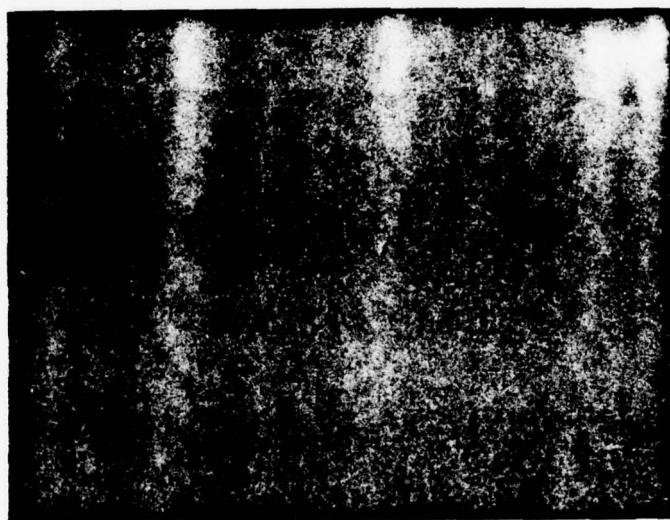


Figure 3. Polished surface of CaF_2 oriented 1° from the (100) crystallographic plane. Nomarski photomicrograph, 305X, Sample No. (100)-28.

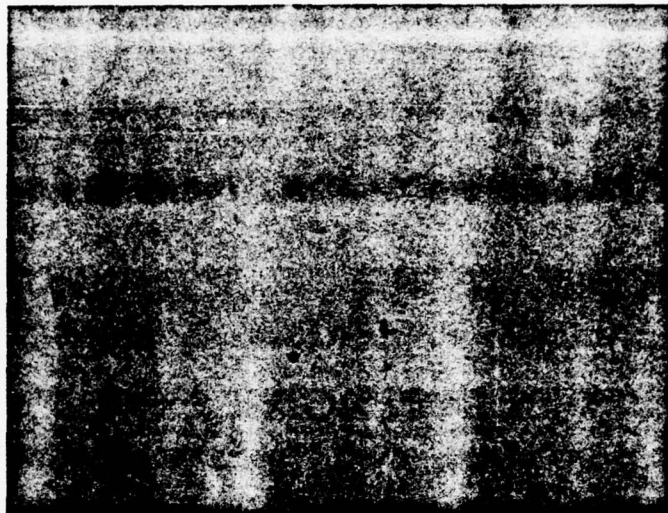


(A)

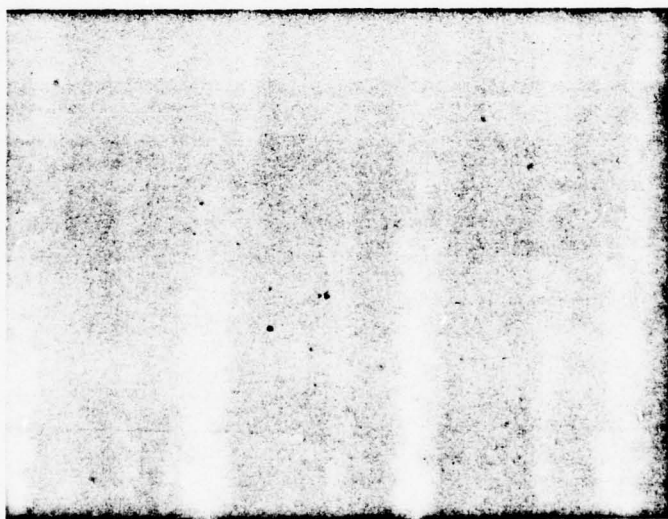


(B)

Figure 4. Polished surfaces of SrF_2 Nomarski photomicrographs (305X). (A) Sample No. (100)-28, oriented 2.5° from (100). (B) Sample No. (110)-28, oriented 0.8° from (110).



(A)



(B)

Figure 5. Polished surfaces of SrF_2 . Nomarski photomicrographs (305X). (A) Sample No. (111)-28, oriented 0.8° from (111). (B) Sample No. (112)-10 oriented parallel to (112).

was suggested as a solution to this problem. Present results indicate that this is correct, but quantitative documentation will require surface roughness measurements.

4. SUBSTRATE ABSORPTANCE MEASUREMENT

In order to obtain absorptance values (β and k) for halfwave thicknesses of coating materials, absorptances for the uncoated substrates must be known. The determination of the absorption coefficient of a coating material on a substrate which is transparent in the wavelength region of the irradiating laser is in principle quite straightforward. The total absorption due to a coating of specified thickness is obtained as a difference in total absorption between coated and uncoated substrates. Sequential measurements on the same substrate are utilized to obtain either a difference in absorption between coated areas or a difference in absorption in a single location before and after coating. The former method has the advantages of speed and ease of verification, but substrate inhomogeneity can cause difficulties. In the latter method, substrate inhomogeneity is eliminated, but verification of the absorption measurement on the uncoated substrate is problematic.

For an uncoated transparent substrate irradiated by a laser beam in a standard adiabatic calorimeter configuration, the total absorption A_o is given by⁽²⁾

$$A_o = \frac{2n_s}{1 + n_s^2} P_A / P_T \quad (1)$$

where n_s is refractive index of the sample, P_A is power absorbed by the sample, and P_T is the power transmitted through the sample. If the masses and heat capacities of the sample and calorimeter cone are known and irradiation times are held constant for a given series of measurements, the absorption is proportional to the ratio of output voltages from the sample and power cone thermocouples.

The total absorptance calculated from (1) includes both surface and bulk contributions. The absorption coefficient for this substrate is

$$\beta = A_o / \ell \quad (2)$$

where ℓ is the sample thickness; again, both surface and bulk contributions are included. If a coating is subsequently deposited upon such a substrate and a new absorption measurement made, the total absorptance takes on a value

$$A_t = A_o + A_1 \quad (3)$$

where A_1 is the increase in total absorptance due to the coating alone. For the case of a coating of halfwave optical thickness, A_1 can be evaluated using (1) and (3) since the surface reflectivity of the coated sample is identical to that of the uncoated substrate and the parenthetical factor involving n_s in (1) remains unchanged.

To obtain an absorption coefficient for a coating of physical thickness t_1 from a measured value of A_1 , we employ a formula of Loomis,⁽³⁾ with minor rearrangement,

$$\beta_1 = \frac{A_1 n_1}{2 t_1 n_o} \frac{(n_o + n_s)^2 \cos^2 \varphi_1 + [n_1 + (n_o n_s / n_1)]^2 \sin^2 \varphi_1}{n_1^2 + n_s^2}, \quad (4)$$

where

n_1 = film refractive index

n_s = substrate refractive index

n_o = incident medium refractive index

$\varphi_1 = 2\pi n_1 t_1 / \lambda_o$

λ_o = laser wavelength (vacuum).

For a single coating of thickness $\lambda_o/2$, (4) reduces to

$$\beta_1 = \frac{A_1 n_1}{2 t_1 n_o} \frac{(n_o + n_s)^2}{n_1^2 + n_s^2} \quad (5)$$

The absorption index of the thin film is then

$$k_1 = \frac{\lambda_o \beta_1}{4\pi} \quad (6)$$

Hence, in order to obtain the absorption coefficient and absorption index of a single layer coating on a transparent substrate, we require only the refractive index of film and substrate, the physical thickness of the film, and two absorption measurements. The method of measuring the absorption has been discussed in the literature. (4, 5)

Measurement of absorptance of uncoated single crystal CaF_2 and SrF_2 substrates will be completed in early January, 1977. Results to date are listed in Tables 11-18. In these tables, the column headed " $A \times 10^4$ " or " $A \times 10^5$ " gives the mean total fraction absorbed by the uncoated substrate in units of 10^{-4} or 10^{-5} . This absorptance includes both surface and bulk contributions. The dual column headed "Standard Deviation" gives the standard deviation of five or more measurements both in units of 10^{-4} or 10^{-5} and as a percent of the mean.

The problem of experimental dispersion (i.e., high standard deviation) in the the results noted in the First Quarterly Report has largely been solved for measurements at both CO and DF wavelengths. The solution involved improvement of the sample chamber vacuum by replumbing to the vacuum pump, rewiring the thermocouple feedthrough, and cooling of the calorimeter cone by airflow between runs. The latter procedure had the greatest effect due to reduction in heatflow from the surroundings to the sample by conductive and/or radiative processes. Improvement of vacuum also aided in

Table 11. TOTAL ABSORPTANCE OF UNCOATED
(100) CaF_2 SUBSTRATES AT 5.3 μm .

SAMPLE NO.	$A \times 10^4$	STANDARD DEV.	
		$\times 10^4$	%
1	2.85	0.17	5.85
21	2.85	0.10	3.60
24	2.37	0.09	3.87
25	2.50	0.12	4.94
26	3.27	0.12	3.74
27	2.32	0.05	2.02

Table 12. TOTAL ABSORPTANCE OF UNCOATED
(100) CaF_2 SUBSTRATES AT $3.8 \mu\text{m}$.

SAMPLE NO.	$A \times 10^5$	STANDARD DEV.	
		$\times 10^5$	%
2	8.85	0.19	2.19
3	8.95	0.42	4.75
6	9.90	0.23	2.36
7	8.69	0.38	4.41
9	8.11	0.29	3.59
10	9.65	0.68	7.00
11	6.17	0.22	3.49
13	7.93	0.19	2.43
14	6.68	0.24	3.55
22	10.66	0.62	5.80
23	11.32	0.42	3.76

Table 13. TOTAL ABSORPTANCE OF UNCOATED
(110) CaF_2 SUBSTRATES AT $5.3\mu\text{m}$.

SAMPLE NO.	$A \times 10^4$	STANDARD DEV.	
		$\times 10^4$	%
(110) -1	2.92	0.15	5.28
2	0.904	0.009	0.96
3	3.05	0.10	3.28
5	3.63	0.17	4.62
6	2.98	0.12	3.91
10	3.96	0.19	4.88
25	2.75	0.07	2.47
27	3.70	0.06	1.72

Table 14. TOTAL ABSORPTANCE OF UNCOATED
(110) CaF_2 SUBSTRATES AT $3.8\mu\text{m}$.

SAMPLE NO.	$A \times 10^4$	STANDARD DEV.	
		$\times 10^4$	%
4	0.951	0.029	3.00
8	1.19	0.07	5.57
9	1.38	0.10	6.90
12	0.822	0.063	7.63
13	3.91	0.15	3.84
14	1.17	0.09	7.45
16	1.02	0.03	2.87
19	1.35	0.10	7.38
23	1.12	0.04	3.95
24	1.07	0.06	5.62
26	1.03	0.06	5.50
28	1.03	0.03	2.94

Table 15. TOTAL ABSORPTANCE OF UNCOATED
(111) CaF_2 SUBSTRATES AT $5.3 \mu\text{m}$.

SAMPLE NO.	$A \times 10^4$	STANDARD DEV.	
		$\times 10^4$	%
1	2.82	0.32	11.30
2	2.77	0.27	9.84
3	2.64	0.11	4.25
4	2.44	0.11	4.58
5	3.56	0.09	2.43
6	3.56	0.14	3.93
7	3.07	0.10	3.13
8	2.88	0.08	2.71
9	3.54	0.13	3.72
10	5.32	0.13	2.49

Table 16. TOTAL ABSORPTANCE OF UNCOATED
(111) CaF_2 SUBSTRATES AT $3.8 \mu\text{m}$.

SAMPLE NO.	$A \times 10^4$	STANDARD DEV.	
		$\times 10^4$	%
11	0.907	0.074	8.17
12	1.09	0.09	8.28
13	1.22	0.07	5.68
14	0.729	0.098	13.47
15	0.947	0.072	7.56
16	1.43	0.08	5.32
17	1.43	0.03	2.23
18	1.04	0.06	5.37
19	1.07	0.05	5.01
20	1.40	0.07	5.32
21	0.958	0.043	4.46
28	0.806	0.043	5.38

Table 17. TOTAL ABSORPTANCE OF UNCOATED
(100) SrF_2 SUBSTRATES AT $5.3 \mu\text{m}$.

SAMPLE NO.	$A \times 10^5$	STANDARD DEV.	
		$\times 10^5$	%
1	4.06	0.26	6.31
2	5.90	0.35	5.97
3	3.35	0.07	2.11
4	4.07	0.11	2.80
6	3.38	0.08	2.48

Table 18. TOTAL ABSORPTANCE OF UNCOATED
(100) SrF_2 SUBSTRATES AT $3.8 \mu\text{m}$.

SAMPLE NO.	$A \times 10^5$	STANDARD DEV.	
		$\times 10^5$	%
7	9.13	0.18	1.96
8	9.52	0.31	3.29
9	13.43	0.54	4.00
10	10.27	0.51	5.01
14	11.05	0.45	4.09
15	9.47	0.30	3.18
16	6.73	0.23	3.38
17	8.79	0.22	2.52
18	9.01	0.18	1.97
19	8.13	0.25	3.07

reducing conductive heat flow, while rewiring of the thermocouple feed-through markedly reduced high frequency noise.

With regard to absolute magnitude of the results, note that for CaF_2 , the absorptance at $3.8 \mu\text{m}$ is generally lower, by a factor of 2 or 3, than it is at $5.3 \mu\text{m}$. Standard deviations are of the order of 1×10^{-5} or less for this material. Since typical $5.3 \mu\text{m}$ absorptances for $\lambda/2$ coatings on CaF_2 substrates are of the order of ⁽⁶⁾ 8 or 9×10^{-5} , subsequent measurements of absorptance of coated samples and determination of coating absorptance by subtraction should permit determination of coating absorptances to within $\pm 25\%$.

For SrF_2 , absorptance at $3.8 \mu\text{m}$ is about double that at $5.3 \mu\text{m}$ (Tables 17 and 18). Standard deviations are of the order of 2 to 5×10^{-6} , which should permit determination of coating absorptances to within $\pm 10\%$ if these values are similar to those on CaF_2 substrates.

To examine these results in the light of intrinsic values, it is instructive to calculate a total β (including surface and bulk contributions) for the two materials, two wavelengths, and various orientations for which data are presently available. Results of such calculations are listed in Table 19. In this table, the column headed " $\bar{\beta}(\text{cm}^{-1})$ " gives the mean of all values of β for all samples of a given material and orientation measured under this program at the specified wavelength. Each value of β used to calculate the mean was obtained by dividing a total absorptance (A) by sample thickness and hence includes surface and bulk contributions. Each mean value listed in the table is an average of results for six to twelve samples. The dispersion (i.e., standard deviation) of results noted in Table 19 is an indication of the range of values for the number of samples tested, rather than of experimental error.

Table 19. MEAN TOTAL ABSORPTION COEFFICIENT
(β) FOR CaF_2 AND SrF_2 AT 5.3 AND 3.8 μm .

MATERIAL	ORIENTATION	λ (μm)	$\bar{\beta}$ (cm^{-1})
CaF_2	(100)	5.3	$(4.05 \pm 0.55) \times 10^{-4}$
	(110)	5.3	$(4.42 \pm 1.51) \times 10^{-4}$
	(111)	5.3	$(5.02 \pm 1.06) \times 10^{-4}$
	(100)	3.8	$(1.28 \pm 0.23) \times 10^{-4}$
	(110)	3.8	$(1.92 \pm 1.21) \times 10^{-4}$
	(111)	3.8	$(1.56 \pm 0.27) \times 10^{-4}$
SrF_2	(100)	5.3	$(6.79 \pm 1.68) \times 10^{-5}$
		3.8	$(1.56 \pm 0.29) \times 10^{-4}$

The results of Table 19 are plotted in Figure 6, along with those of Harrington.⁽⁷⁾ For comparison, lines indicating intrinsic values obtained by Deutsch⁽⁸⁾ are also plotted for both materials. It is clear from this plot that values for CaF_2 at $5.3 \mu\text{m}$ (CO) are near intrinsic, while at $3.8 \mu\text{m}$ (DF) and $2.8 \mu\text{m}$ (HF) they are definitely extrinsically controlled. For SrF_2 at $5.3 \mu\text{m}$, the value is about three times the expected intrinsic. At $3.8 \mu\text{m}$, the absorption coefficient of SrF_2 is essentially equivalent to that of CaF_2 , exceeding the intrinsic value by several orders of magnitude. At HF wavelengths the situation for both CaF_2 and SrF_2 is similar, in that both coefficients exceed intrinsic values by many orders of magnitude.

The origin of the extrinsic values and the chemical nature and location of the atomic species responsible are not obvious from present data. It is clear that surface effects in the CO wavelength region are more easily recognized in SrF_2 than in CaF_2 due to the lower intrinsic level in the former material. It is also apparent that similar contaminants are responsible for the extrinsically controlled absorptance in both CaF_2 and SrF_2 , since the absolute levels are almost identical.

5. SUBSTRATE SURFACE CHEMISTRY AND CLEANING

To establish effects of various cleaning procedures upon substrate surface chemistry and absorptances, an investigation comprising parallel Auger Electron Spectroscopy and laser calorimetry studies was carried out on CaF_2 , the only sample material available. Results of this investigation were presented at the recent Topical Meeting on Optical Phenomena in Infrared Materials (Optical Society of America) and will be published in Applied Optics. A copy of the manuscript is appended to this report.

6. FUTURE PLANS

Work during the next two quarters will concentrate on single layer coating deposition and determination of structure and properties, the data-gathering phase of the effort. A revised schedule, taking into account the late substrate material deliveries, follows.

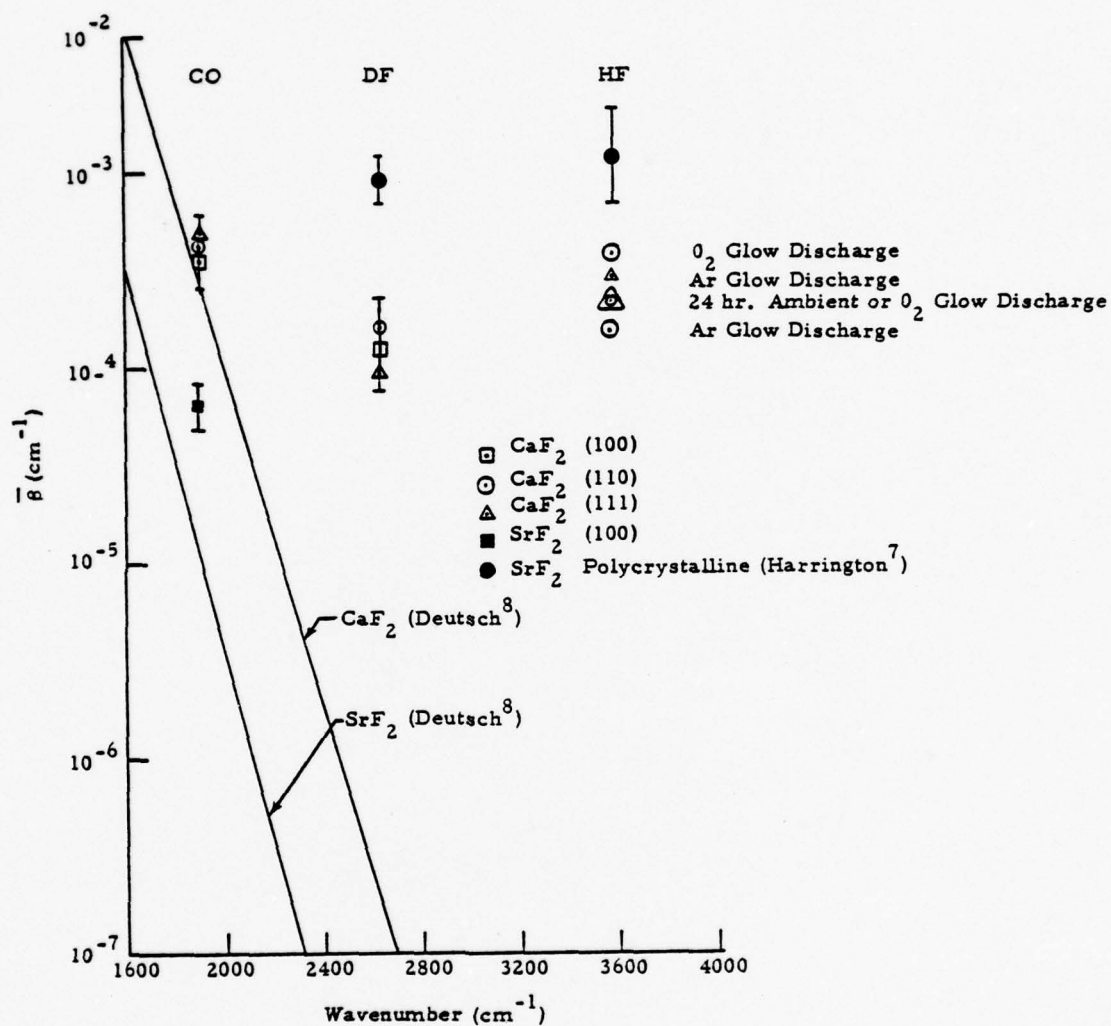
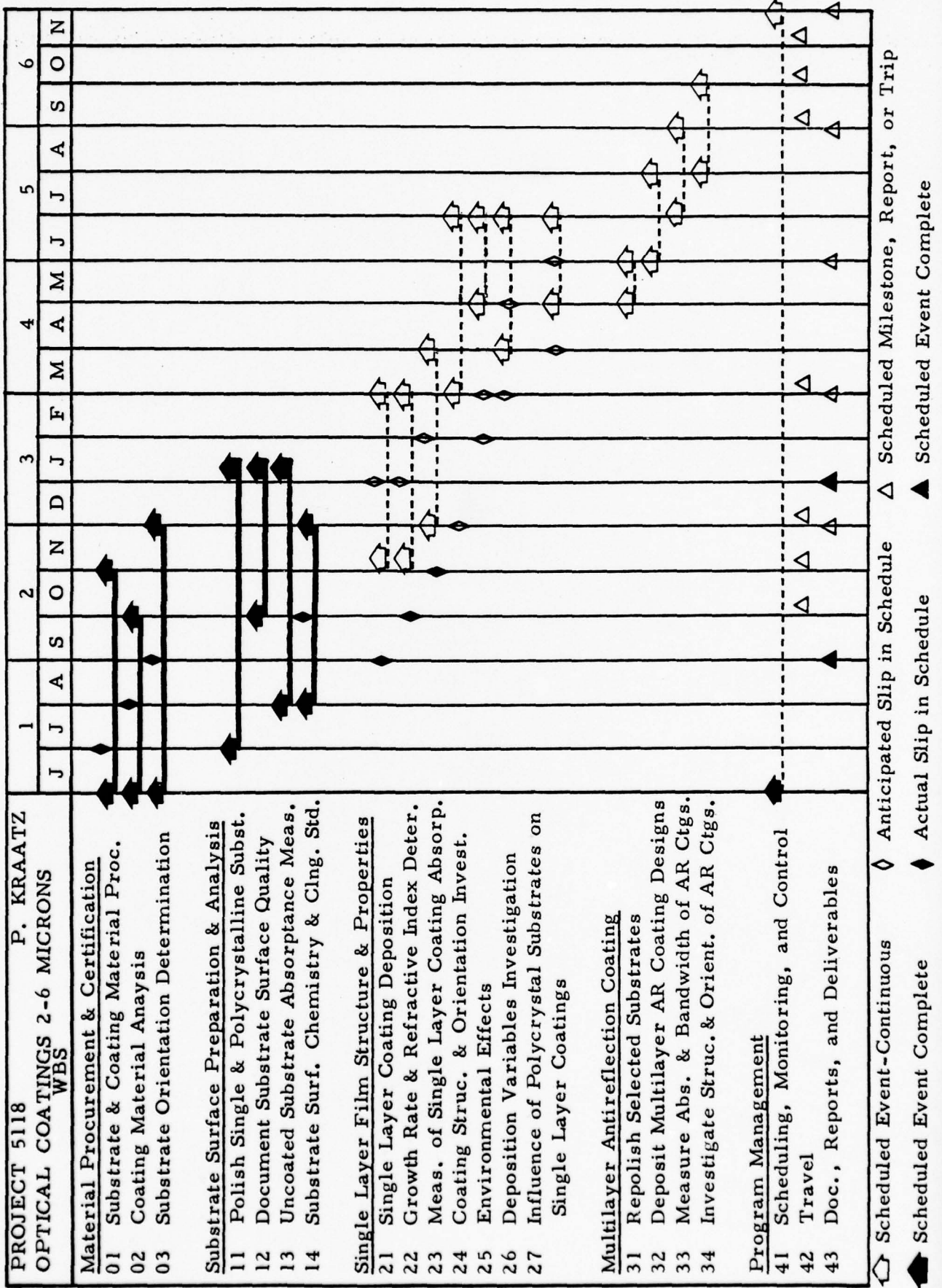


Figure 6. Mean Total Absorption Coefficient ($\bar{\mu}$) vs. Wavenumber for CaF_2 and SrF_2 .



7. REFERENCES

1. S. J. Holmes and P. Kraatz, "Investigation of Crystal Orientation Influence on Thin Film Coatings for CaF_2 Laser Windows," Final Technical Report, Northrop Research and Technology Center, 1 October 1975, Contract No. F33615-75-C-5190, Air Force Materials Laboratory, Ohio.
2. R. Weil, "Calculations of Small Absorption Coefficients From Calorimetric Experimental Data", J. Appl. Phys., Vol. 41, p. 3012, (1970).
3. J. S. Loomis, "Absorption in Coated Laser Windows", Appl. Opt., Vol. 12, p. 877, (1973).
4. P. Kraatz, and P. J. Mendoza, "CO Laser Calorimetry for Surface and Coating Evaluation", Proc. Fourth Conference on Infrared Laser Window Materials, p. 77, 1975.
5. T. F. Deutsch, "Research in Optical Materials and Structures for High Power Lasers," Final Technical Report, Raytheon Research Division, ARPA Order 1180 (1973).
6. P. Kraatz, S. J. Holmes, and A. Klugman, "Absorptance of Coated Alkaline Earth Fluoride Windows at CO Laser Wavelengths" Proc. of the Fifth Conference on Infrared Laser Window Materials, C. Robert Andrews and Charles L. Strecker, Eds. AFML, 1976.
7. J. A. Harrington, "Low Loss Windows for Chemical Lasers", Semi-Annual Technical Report, Contract No. DAAH01-74-C-0437, ARPA Order 2614, August 1975.
8. T. F. Deutsch, "Absorption Coefficient of Infrared Laser Window Materials" J. Phys. Chem. Solids 34, 2091-2104, 1973.

APPENDIX

SURFACE CHEMISTRY
AND ABSORPTANCE OF
 CaF_2 AT HF, DF AND CO
WAVELENGTHS*

P. KRAATZ AND S. J. HOLMES
NORTHROP CORPORATION
Northrop Research and Technology Center
Hawthorne, California 90250

ABSTRACT

The relative importance of bulk and surface contributions to absorptance in transmitting optics at DF and CO wavelengths has recently been discussed, with the observation that the surface contribution may be as much as 15 times that of the bulk.¹ The nature of changes in surface absorption and surface chemistry associated with such processes as cleaning with organic solvents² or vacuum glow discharge have not been fully explained.^{1,2} To elucidate some aspects of these problems, we report results of some investigations employing Auger electron spectroscopy (AES) in conjunction with HF, DF, and CO laser calorimetry. It has been found that the effects of vacuum glow discharge cleaning and subsequent exposure to ambient atmosphere vary markedly with the nature of the gas employed (reactive, e.g. Oxygen, or inert, e.g. Argon) and with the crystallographic orientation and specific surface free energy of the sample surfaces, as well with the laser wavelength employed in calorimetric measurements. Results of experiments in which these parameters are varied are discussed in the light of parallel AES studies.

*Work supported by DARPA under Navy Contract No. N00123-76-C-1321.

INTRODUCTION

Processes contributing to changes in the surface component of absorptance of the alkaline earth fluorides in the middle infrared region of the spectrum are not well understood.^{1,2} Various solvent cleaning procedures, as well as vacuum glow discharge and exposure to the ambient atmosphere may profoundly influence this property in wavelength regions of interest for high power chemical (HF, DF) and CO lasers operating nominally at 2.8, 3.8, and 5.3 μm , respectively. In the present work, elucidation of some effects of glow discharge cleaning in an Argon or Oxygen medium, with subsequent exposure to the ambient atmosphere is attempted, utilizing laser calorimetry at HF, DF, and CO wavelengths and Auger electron spectroscopy. In addition, the influence of crystallographic orientation of sample surfaces upon response to these processes is illustrated. Results are discussed in terms of elemental composition of surfaces, their atomic configuration, and specific surface free energy.

2. EXPERIMENTAL METHODS

The laser absorption vacuum calorimeter used to obtain the present Absorptance data was constructed following the general design of Deutsch³ and has been described in detail elsewhere.⁴ The only change in the apparatus since the

previous description has been the addition of a CW HF/DF chemical laser and suitable AR coated windows for the calorimeter box when working at the chemical laser wavelengths. The chemical laser itself has also been described in detail elsewhere.⁵ Maximum available DF power is 11 Watts, but 1 to 3 Watts was sufficient for calorimetric measurements on the small (1 in. diameter x 1/4 in. thick) samples employed in this study. An irradiation time of 2 to 3 minutes at these power levels was adequate for absorbance measurement. The calorimeter is liquid nitrogen trapped and was evacuated to a pressure of 0.08 to 0.15 Torr during measurements. Samples were irradiated at 3 different wavelengths in succession without breaking vacuum, in an absorbance determination comprising irradiation with HF, DF, and CO lasers.

Auger electron spectroscopy (AES) analyses were carried out in a Physical Electronics unit equipped with a sputter ion gun capable of sputter etching a specimen while simultaneously monitoring the AES signal. Since this system must operate in a vacuum of 10^{-9} to 10^{-10} Torr, pumpdown times are substantial, placing a practical lower limit of about 12 hours on the interval between analyses of samples exposed to different environmental conditions. Samples for Auger analysis were subjected to the various surface processing operations simultaneously with those samples

prepared specifically for absorptance measurements and were exposed to the ambient (laboratory) atmosphere for comparable total times following these operations.

All AES analyses were carried out with a primary 2 keV electron beam to avoid problems of surface charge buildup on the insulating CaF_2 samples. Even at this low beam energy, simultaneous sputter etching and AES profiling could be carried only to depths of a few hundred Ångströms due to charge build-up and resultant peak displacement. Auger peaks for Calcium and Fluorine and common surface contaminants such as Oxygen, Nitrogen and Sulfur were monitored. The carbon peak, which is of intense interest in a study of this nature, unfortunately could not be resolved due to its proximity to the large calcium peak on CaF_2 surfaces. Repetition of the experiments on SrF_2 surfaces would be useful in this regard.

prepared specifically for absorptance measurements and were exposed to the ambient (laboratory) atmosphere for comparable total times following these operations.

All AES analyses were carried out with a primary 2 keV electron beam to avoid problems of surface charge buildup on the insulating CaF_2 samples. Even at this low beam energy, simultaneous sputter etching and AES profiling could be carried only to depths of a few hundred Ångströms due to charge build-up and resultant peak displacement. Auger peaks for Calcium and Fluorine and common surface contaminants such as Oxygen, Nitrogen and Sulfur were monitored. The carbon peak, which is of intense interest in a study of this nature, unfortunately could not be resolved due to its proximity to the large calcium peak on CaF_2 surfaces. Repetition of the experiments on SrF_2 surfaces would be useful in this regard.

Surface cleaning processes investigated in the present work are similar to those employed previously.^{1,2} They comprise a solvent cleaning procedure and glow discharge cleaning procedure. These may be described briefly as follows:

Solvent Cleaning Procedure

- (1) Soak in acetone (30 minutes).
- (2) Rinse with warm tap water.
- (3) Wash with warm tap water and liquid detergent.
- (4) Rinse with distilled water.
- (5) Rinse with reagent grade alcohol.
- (6) Blow dry with nitrogen gas.

Glow Discharge Cleaning Procedure

- (1) Solvent clean, as above, place in vacuum chamber.
- (2) Pump out chamber to $\sim 5 \times 10^{-6}$ Torr (1 Hr.). Heater on (200°C).
- (3) Glow discharge 3 minutes at 200 mA in 2×10^{-2} Torr of Argon.
- (4) Heater off. Valve shut. (10^{-4} Torr range).
- (5) Sample cools to ambient (1 Hr.).
- (6) Remove sample from glow discharge chamber, place in laser calorimeter following equilibration to room temperature (20-30 min.).
- (7) Pump out calorimeter

In a variation of the argon glow discharge procedure to test the effect of a reactive atmosphere, oxygen was substituted for argon, with all other parameters held constant.

The basic experiments reported here involved solvent cleaning of two groups of samples, followed by calorimetric absorbance measurement and Auger electron spectroscopy. One group of samples was subsequently glow discharge cleaned in an argon medium and the other in an oxygen medium. Following these processes, changes in

absorptance with exposure to ambient atmosphere were monitored at HF($2.8\text{ }\mu\text{m}$), DF($3.8\text{ }\mu\text{m}$) and CO($5.3\text{ }\mu\text{m}$) wavelengths. Elemental composition of sample surfaces was monitored with AES. Argon ion milling within the Auger system was utilized to determine the depth of coverage and tenacity of contaminant species upon CaF_2 surfaces. Each group of samples was composed of equal numbers of (111) and (110) orientations to determine the influence of crystallographic orientation upon contaminant composition and optical absorption.

RESULTS

Effects of Argon glow discharge cleaning upon optical absorptance are illustrated in Table I and figures 1 and 2. In these figures, each symbol represents the mean of 5 or more absorptance measurements with error bars representing the experimental dispersion (standard deviation). Symbols lacking error bars represent results in which experimental dispersion plots within the size of the symbol employed.

At $5.3\text{ }\mu\text{m}$, total absorptance (β_T) of samples with surfaces oriented parallel to (111) decreases approximately 25% relative to the solvent-cleaned value after 0.5 and 4.5 hours exposure to ambient atmosphere. The apparent decrease is approximately 31% following 22 hours exposure, but this difference is not significant due to experimental dispersion. At $3.8\text{ }\mu\text{m}$, the initial decrease is approximately 43% going to 38% in 4.5 hours and 57% in 22 hours. The latter decrease is statistically significant. At $2.8\text{ }\mu\text{m}$, we see a 20% decrease, relative to the freshly glow discharge cleaned value, in 4.5 hours remaining constant over 22 hours exposure to ambient atmosphere.

For samples with surfaces oriented parallel to (110), behavior is quantitatively and qualitatively different. At $5.3\text{ }\mu\text{m}$, glow discharge cleaning produces an immediate decrease of 12%, followed by an increase of 21% after 6 hours

exposure, relative to the value for the solvent cleaned sample. After 24 hours, the absorptance is within 9% of the solvent cleaned value. At $3.8\text{ }\mu\text{m}$, an initial decline of 47% is followed by an increase of 41% after 6 hours exposure relative to the solvent cleaned sample. At 24 hours, the absorptance is 7% below the value for the solvent cleaned sample, which is within the standard deviation of the measurements. At $2.8\text{ }\mu\text{m}$, the absorptance increases by 86%, relative to the freshly glow discharged condition, within 6 hours. The absorptance subsequently decreases to within 57% of this value after 24 hours exposure. For both crystallographic orientations, highest absorptances are at $5.3\text{ }\mu\text{m}$ and $2.8\text{ }\mu\text{m}$, while the lowest absolute values and greatest initial decreases are seen at $3.8\text{ }\mu\text{m}$, for glow discharge cleaning in an inert gas.

Results for a similar series of experiments, utilizing a reactive glow discharge medium (oxygen) are shown in Table II and figures 3 and 4. It is clear that these results differ radically from those in which an inert glow discharge medium was employed and again the response of (111) and (110) surfaces differs markedly. In all cases absorptance at $2.8\text{ }\mu\text{m}$ is greatest, followed by $5.3\text{ }\mu\text{m}$, while that at $3.8\text{ }\mu\text{m}$ is a minimum.

On (111) surfaces of CaF_2 , $5.3\text{ }\mu\text{m}$ absorptance decreases approximately 21%, relative to the solvent cleaned value, after oxygen glow discharge and 3 hours exposure to ambient. This decrease is essentially constant at 26% after 20 hours. At $3.8\text{ }\mu\text{m}$, the corresponding values are 46% and 50% decreases, respectively. At $2.8\text{ }\mu\text{m}$, absorptance values after 3 hours and 20 hours ambient exposure are indistinguishable, within experimental precision.

On (110) surfaces of CaF_2 , the situation is entirely different: At $5.3\text{ }\mu\text{m}$, absorptance increases by 11% within 20 minutes after oxygen glow discharge cleaning and remains 3% higher than the solvent cleaned value after 20 hours. At $3.8\text{ }\mu\text{m}$, an initial decrease of 3% becomes 27% after 20

hours exposure to ambient. At $2.8\mu\text{m}$, values are again high and essentially indistinguishable after 20 minutes or 20 hours.

Auger results are most conveniently expressed in terms of the ratio of oxygen to calcium peak heights, since oxygen is probably the most directly related to mid IR absorptance of the elements monitored. (As noted previously, Carbon could not be monitored due to masking by the calcium peak.) In general, all AES traces showed sulfur, nitrogen, oxygen, and strontium in addition to calcium and fluorine in scans of surfaces which were either solvent or glow discharge cleaned with Argon before insertion in the system. Nitrogen was absent from samples exposed to oxygen glow discharge. Argon ion milling to a depth of a few hundred Ångstroms within the AES system removed sulfur and nitrogen in all cases and significantly changed the relative peak height of oxygen in some cases, to be discussed later. The strontium peak height was unchanged by ion milling, indicating that it is a bulk impurity in the CaF_2 .

Oxygen to calcium ratios are shown in table III for solvent cleaned samples and those subjected to Argon or oxygen glow discharge. Results for Argon glow discharge cleaning are plotted in figure 5 and for oxygen glow discharge in figure 6. Error bars represent the approximate $\pm 10\%$ expected precision in the experimental O/Ca ratios. Comparison with absorptance results plotted in figures 1 - 4 shows poor correlation, except in isolated cases; e. g. the 20% reduction in O/Ca ratio on (111) CaF_2 following oxygen glow discharge cleaning is similar to the 21% reduction in absorptance at $5.3\mu\text{m}$ shown in table II. In general, the trend of the Auger results is toward increasing O/Ca ratio with time of exposure to ambient, except in the case of (110) CaF_2 surfaces subjected to Argon glow discharge cleaning, which show a decrease. Most changes, however, are not significant relative to the solvent cleaned or initial glow discharge values, when experimental dispersion is taken into account.

On the other hand, the results of profiling surfaces using Argon ion milling within the Auger system are more interesting. Results of this operation are illustrated in Table IV. Due to the highly insulating character of the CaF_2 surfaces, monitoring of AES peaks during ion milling was precluded by static charging effects in all but the single case noted in table IV. Hence, it was necessary to take an initial and final scan following the milling operation. The final scan thus does not accurately represent the uncontaminated CaF_2 surface, since some oxygen is redeposited in the time (5-10 minutes) required for stabilization of the charged surface. However, the amount of oxygen redeposited apparently differs markedly with the nature of the crystal surface and its history.

For example, we see that for (110) surfaces subjected to Argon glow discharge cleaning and 1/2 hour in the ambient atmosphere, the final O/Ca ratio after milling is reduced by a factor of four below the initial value. On the other hand for (111) surfaces treated similarly, the reduction is by a factor of ten. For Argon glow discharged (110) surfaces exposed to the ambient for 26 hours, a net increase in O/Ca ratio follows ion milling on (110) and a reduction by a factor of two occurs on (111). For oxygen glow discharged (110) surfaces with 1/2 hour ambient exposure, the decrease is by a factor of only 1.6, while for (111) there is a slight, but insignificant increase. For oxygen glow discharged surfaces exposed to ambient for 30 hours, the maximum decrease is only 36% on a scan taken during milling. A final scan for the (111) surface could not be obtained.

DISCUSSION

Optical absorbance of CaF_2 in the middle infrared, as determined by laser calorimetry at 2.8, 3.8, and 5.3 μm , is found to vary significantly with the nature of the glow discharge medium (reactive or inert), time of subsequent exposure to the ambient atmosphere, and the crystallographic orientation of the optical surfaces tested. These changes show no real correlation with surficial O/Ca ratios

determined by AES, indicating either that the differences arise from contaminants other than oxygen (e. g. hydrocarbons) or that they arise from variations in the state of aggregation of oxygen atoms on the surfaces. Ion milling experiments provide tentative evidence favoring the latter hypothesis.

Differences in behavior with crystallographic orientation are most readily examined in relation to the details of structure and physical properties of those surfaces. The arrangement of atoms in the (111) and (110) surfaces of CaF_2 is illustrated in figure 7, taken from Phillips.⁶ In this figure, the large circles represent fluorine ions and the small circles represent calcium ions. The (111) surface is the natural cleavage plane of CaF_2 and is thus electrically neutral.⁷ Examination of experimentally determined electron density distributions in CaF_2 shows overlap between F^- ions in the [100] and [110] directions, but none in the [111] direction,⁸ indicating that the breaking of bonds in the former two directions gives rise to free charges while breaking of [111] bonds does not. In addition, consideration of the specific surface free energy (i. e. the energy required to create new surface of unit area by a reversible process of cutting) of (111) and (110) surfaces of CaF_2 indicates that the surface energy of the (110) surface is approximately double that of the (111) surface.⁹ Hence, we may conclude that the (110) surface of CaF_2 is more reactive than the (111) surface. This is also supported by the ion milling results reported in Table IV.

Time dependence of absorptance upon exposure to ambient atmosphere may be explained using these properties of the surfaces involved. Following Argon glow discharge cleaning, (111) CaF_2 surfaces are covered with an oxygen-rich layer which is not too tightly bound, as indicated by the AES results in Tables III and IV. Due to their electrical neutrality, they do not react rapidly with oxygen of the ambient atmosphere. As a consequence, they show no significant increase in absorptance with exposure to ambient atmosphere (fig. 1).

On the other hand, (110) CaF_2 surfaces subjected to an identical process are covered with a more tenacious oxygen-rich layer and react more rapidly with oxygen, as indicated by the data of tables III and IV. Thus, their surfaces are apparently activated by the glow discharge cleaning and react rapidly with oxygen of the ambient atmosphere. Hence, the optical absorptance of these samples increases to a maximum at some point within less than 24 hours following glow discharge cleaning and then decreases to a value approaching that of the solvent cleaned sample in 24 hours. This phenomenon could arise from the formation of more tightly bound and stable oxygen-rich complexes with prolonged exposure of the activated (110) surfaces to the ambient atmosphere. The data of table IV would tend to support this.

An explanation of the oxygen glow discharge effects upon absorptance at (111) and (110) surfaces may be made following similar reasoning. On (111), the process produces an initial decrease in absorptance which remains constant with exposure to ambient, reflecting the relatively non-reactive nature of the surface and the stability of the oxygen-rich complexes formed there (Table IV). On (110), no significant initial decrease in absorptance is produced by the glow discharge, due to the immediate saturation of available bonding sites at the surface and rapid formation of relatively tightly bound and stable oxygen-rich complexes. This is again supported by the data of Table IV. The high absorptance at the $2.8\text{ }\mu\text{m}$ wavelength in the oxygen processed sample also tends to support this hypothesis, due to its usual association with absorption by hydrogen-oxygen complexes (OH or "water-band").

CONCLUSIONS

1. Surface absorptance of CaF_2 in the mid-infrared is influenced by the amount and state of aggregation of impurities (particularly oxygen) absorbed at the surfaces.

2. The (110) surface is more reactive than (111) and exhibits profound positive and negative changes in absorptance when subjected to glow discharge cleaning in an inert atmosphere (Argon) and subsequent exposure to ambient air. Changes following identical processing of (111) surfaces are less marked, involving only an initial decrease in absorptance followed by relative stability with exposure to ambient atmosphere.
3. Glow discharge cleaning of the reactive (110) surface in a reactive medium (oxygen) produces no marked changes in absorptance at any of the three wavelengths monitored. Identical processing of (111) surfaces produces an initial decrease followed by relative stability, as in the case of Argon glow discharge cleaning noted above.
4. Auger electron spectroscopy is apparently not as sensitive to these changes as is laser calorimetry. However, in combination with ion milling, it can provide useful information on the thickness, stability, and tenacity of surficial contaminants.
5. The role of hydrocarbon contaminants, if any, in these surface chemical reactions remains unknown since carbon could not be monitored in the present work due to overlap with the calcium peak on CaF_2 .

ACKNOWLEDGEMENTS

The authors wish to thank Mr. T. Remmel and Mr. J. Schifando for the Auger measurements and Dr. J. M. Rowe for helpful discussions of the methodology, particularly the sensitivity of laser calorimetry as an analytical tool.

References

1. Rowe, J. M., Kraatz, P., and Holmes, S. J., "Calorimetric Absorptance Measurements of CaF_2 and SrF_2 at DF and CO Wavelengths," Proc. Eighth Symposium on Optical Materials for High Power Lasers, NBS, Boulder, Colorado, (1976).
2. Kraatz, P., Holmes, S. J., and Klugman, A., "Absorptance of Coated Alkaline Earth Fluoride Windows at CO Laser Wavelengths," Proc. Fifth Conf. on IR Laser Window Materials, DARPA, 1975.
3. T. F. Deutsch, "Research in Optical Materials and Structures for High Power Lasers," Final Technical Report, Contract No. DAAH 01-72-C-0194, ARPA Order No. 1180, Raytheon Research Division, 1973.
4. P. Kraatz and P. J. Mendoza, "CO Laser Calorimetry for Surface and Coating Evaluation," Proc. Fourth Conference on Infrared Laser Window Materials, ARPA, 1974.
5. J. A. Harrington, Final Technical Report, Contract No. DAAH 01-74-C-0438, U. S. Army Missile Command, Redstone Arsenal, Alabama, 1975.
6. W. L. Phillips, Jr. "Deformation and Fracture Processes in Calcium Fluoride Single Crystals" J. Amer. Ceramic Soc. 44, 499-506, 1061.
7. L. G. Berry and Brian Mason, MINERALOGY, Freeman, San Francisco, 1959.
8. H. Witte and E. Wölfel, "Electron Distributions in NaCl, LiF, CaF_2 , and Al" Rev. Mod. Phys. 30, 51-55, 1958.

References

9. G. C. Benson and T. A. Claxton, "Calculation of the Surface Energy of the $\{110\}$ Face of Some Crystals Possessing the Fluorite Structure" Canadian Journal of Physics 41, 1287-1293, (1963).

Table I . Optical Absorptance (β_T) of CaF_2 as affected by Solvent Cleaning and Glow Discharge Cleaning with Argon.

SAMPLE ORIENTATION	λ (μm)	$\beta_T (10^{-4} \text{cm}^{-1})$ SOLVENT CLEANED	$\beta_T (10^{-4} \text{cm}^{-1})$ FOLLOWING ARGON GLOW DISCHARGE CLEANING & EXPOSURE TO AMBIENT ATMOSPHERE				
			0.5 HR.	4.5 HR.	5.7 HR.	22.0 HR.	24.0 HR.
(111)	5.3	5.81 ± 0.27	4.33 ± 0.17	4.32 ± 0.29	---	3.99 ± 0.17	---
	3.8	3.19 ± 0.20	1.83 ± 0.05	1.97 ± 0.07	---	1.37 ± 0.14	---
	2.8	---	4.90 ± 0.45	3.95 ± 0.30	---	3.91 ± 0.09	---
(110)	5.3	4.77 ± 0.07	4.18 ± 0.19	---	5.77 ± 0.27	---	4.33 ± 0.17
	3.8	1.81 ± 0.06	0.96 ± 0.02	---	2.55 ± 0.12	---	1.68 ± 0.09
	2.8	---	2.67 ± 0.11	---	4.96 ± 0.28	---	4.20 ± 0.13

NORTHROP
Research and Technology Center

Table II . Optical Absorptance (β_T) of CaF_2 as Affected by Solvent Cleaning and Glow Discharge Cleaning with Oxygen.

SAMPLE ORIENTATION	λ (μm)	(10^{-4}cm^{-1}) SOLVENT CLEANED	$\beta_T (10^{-4} \text{cm}^{-1})$ Following Oxygen Discharge Clean & Exposure to Amb. Atm.		
			0.3 HR.	3.3 HR.	20.5 HR.
(111)	5.3	4.42 ± 0.42	---	3.48 ± 0.21	3.28 ± 0.15
	3.8	3.05 ± 0.18	---	1.66 ± 0.12	1.54 ± 0.17
	2.8	---	---	4.06 ± 0.47	4.37 ± 0.27
(110)	5.3	4.26 ± 0.17	4.74 ± 0.19	---	4.39 ± 0.14
	3.8	4.12 ± 0.18	4.00 ± 0.26	---	3.01 ± 0.08
	2.8	---	6.30 ± 0.28	---	6.12 ± 0.31

NORTHROP
Research and Technology Center

Table III Auger O/Ca Ratio (Peak to Peak) Following Solvent and Glow Discharge Cleaning.

SAMPLE ORIENTATION	O/Ca SOLVENT CLEANED	GLOW DISCHARGE MEDIUM	O/Ca FOLLOWING GLOW DISCHARGE AND EXPOSURE TO AMBIENT ATMOSPHERE		
			0.5 HR.	26.0 HR.	30.0 HR.
(110)	0.3704	ARGON	0.4173	0.2926	---
(111)	0.3576	ARGON	0.3090	0.3963	---
(110)	0.3704	OXYGEN	0.2959	---	0.4230
(111)	0.3576	OXYGEN	0.3128	---	0.5390

NORTHROP
Research and Technology Center

TABLE IV. EFFECT OF ARGON ION MILLING UPON OXYGEN CONCENTRATION ON CaF_2 SURFACES

Surface Orientation	Glow Discharge Medium	Exposure to Ambient (Hr)	O/Ca Initial Scan	O/Ca After Ion Milling
(110)	Argon	0.5	0.4173	0.1016
		26.0	0.2926	0.3282
	Oxygen	0.5	0.2959	0.1853
		30.0	0.4230	0.3097*
(111)	Argon	0.5	0.3090	0.0370
		26.0	0.3963	0.1975
	Oxygen	0.5	0.3128	0.3466
		30.0	0.5390	--

*Scan taken during ion milling.

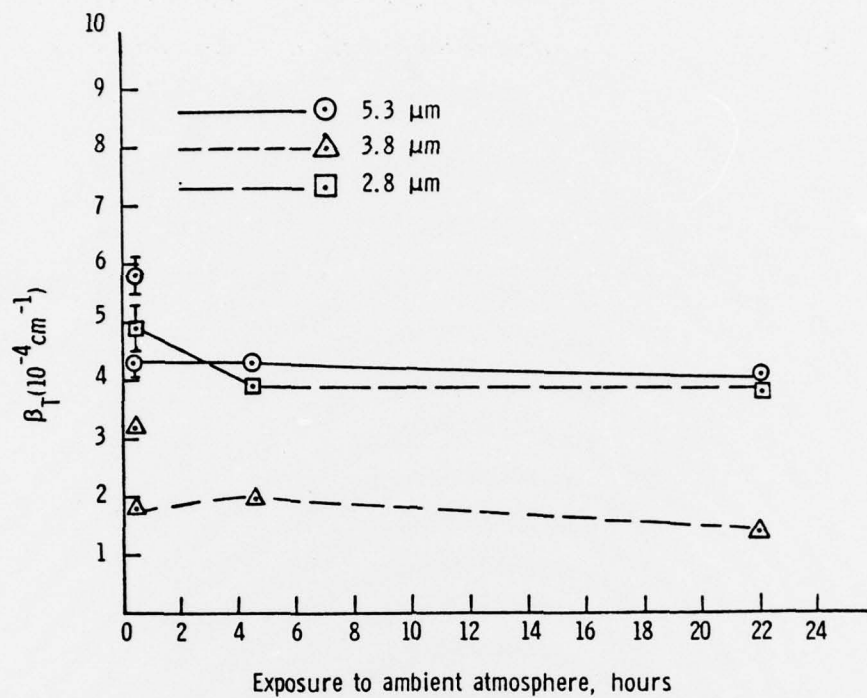


Figure 1 . Changes in Optical Absorptance of (111) CaF_2 Following Argon Glow Discharge Cleaning.

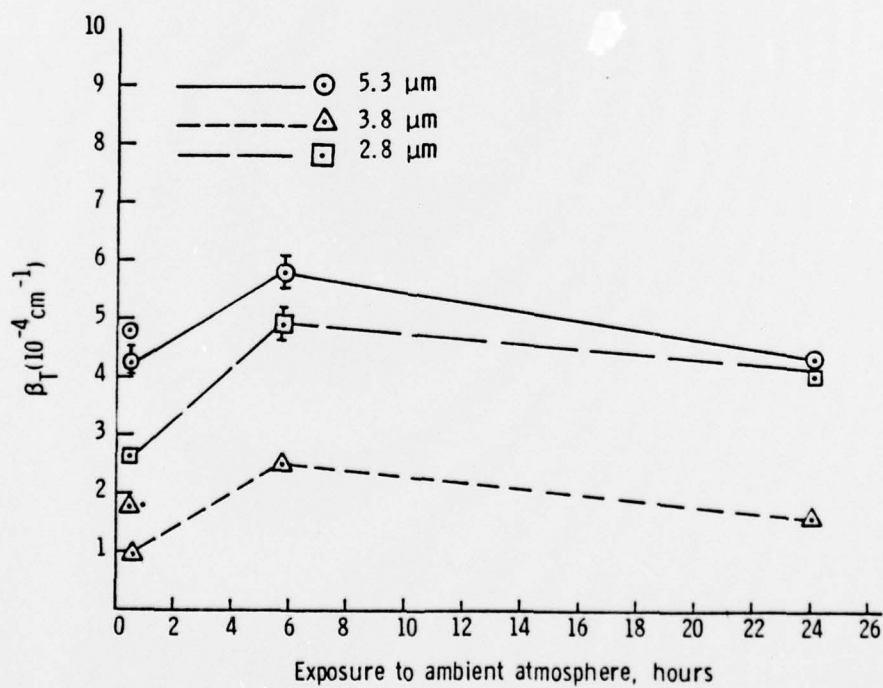


Figure 2. Changes in Optical Absorptance of (110) CaF_2 following Argon Glow Discharge Cleaning.

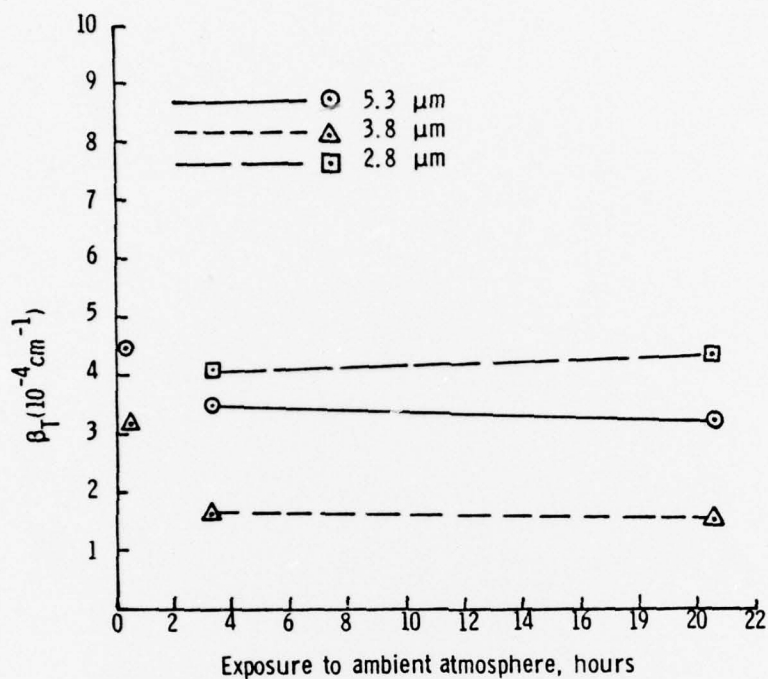


Figure 3 Changes in Optical Absorptance of (111) CaF_2 Following Oxygen Glow Discharge Cleaning.

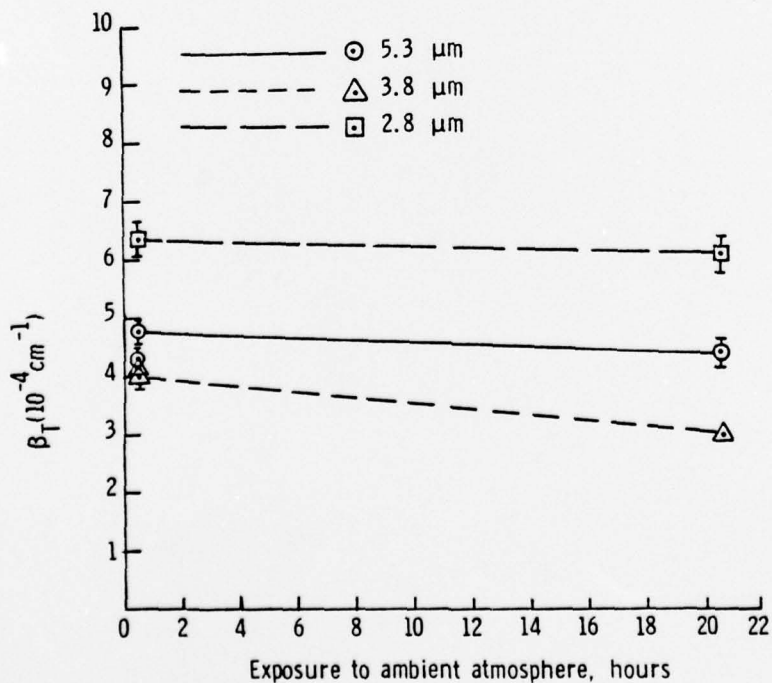


Figure 4. Changes in Optical Absorptance of (110) CaF_2 Following Oxygen Glow Discharge Cleaning.

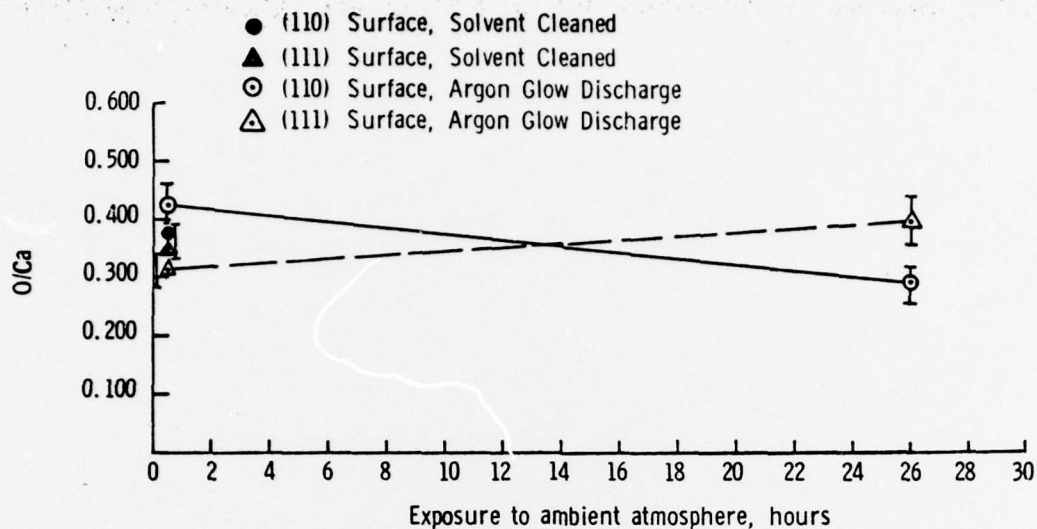


Figure 5. Changes in Auger O/C Ratio (Peak to Peak) with Exposure of CaF_2 Surfaces to Ambient Atmosphere Following Argon Glow Discharge Cleaning.

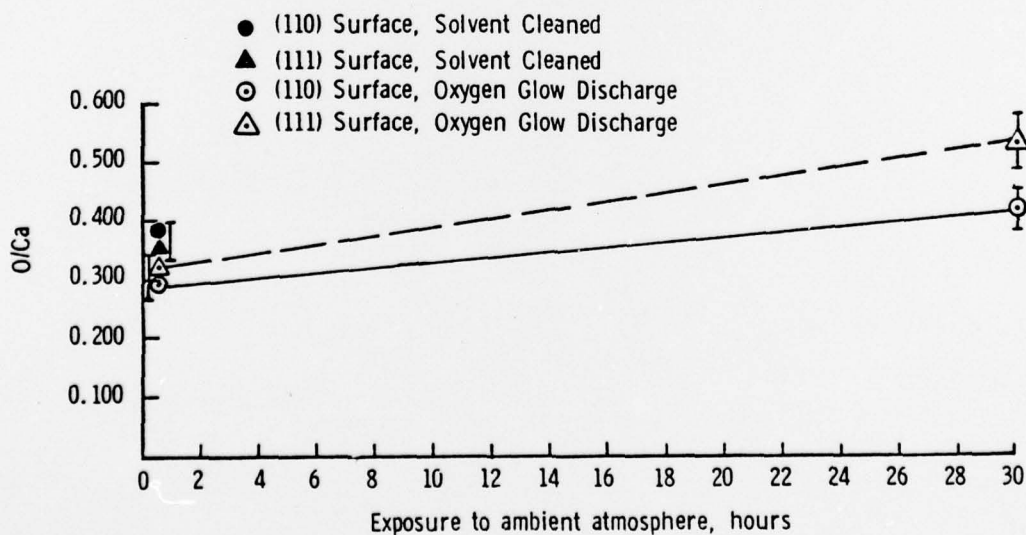


Figure 6. Changes in Auger O/Ca Ratio (Peak to Peak) with Exposure of CaF_2 Surfaces to Ambient Atmosphere Following Oxygen Glow Discharge Cleaning.

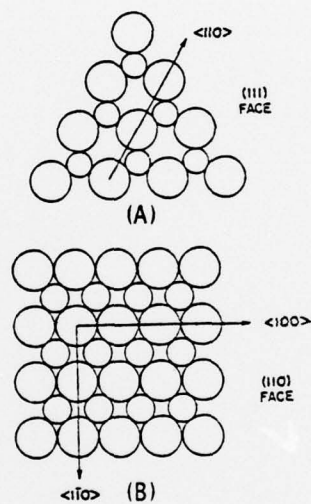


Figure 7 . Atomic Configuration of Two Crystallographic Planes of Calcium Fluoride.

(A) - (111), (B) - (110)

NORTHROP
Research and Technology Center